01 Jan 2023

Observer-based Model Predictive Control With Continuous Control Set For Single-phase Rectifiers

Milad Dehghanzadeh

Rui Bo
Missouri University of Science and Technology, rbo@mst.edu

Kamal Al-Haddad

Recommended Citation

M. Dehghanzadeh et al., "Observer-based Model Predictive Control With Continuous Control Set For Single-phase Rectifiers," *Proceedings of the IEEE International Conference on Industrial Technology*, Institute of Electrical and Electronics Engineers, Jan 2023.
The definitive version is available at https://doi.org/10.1109/ICIT58465.2023.10143042

Observer-based Model Predictive Control with Continuous Control Set for Single-phase Rectifiers

Milad Dehghanzadeh, Rui Bo
Missouri University of Science and Technology
Rolla, USA
milad@mst.edu, rbo@mst.edu

Kamal Al-Haddad
École de Technologie Supérieure
Montreal, Canada
kamal.al-haddad@etsmtl.ca

2023 IEEE International Conference on Industrial Technology (ICIT) | 979-8-3503-3650-4/23/$31.00 ©2023 IEEE | DOI: 10.1109/ICIT58465.2023.10143042

***Abstract*—In this paper, a model predictive controller (MPC) is designed for a single-phase rectifier. The proposed MPC works with a continuous control set (CCS) that addresses variable switching issues in finite control set (FCS) MPCs. The observability of the rectifier enables the design of a full-state observer to measure only output voltage in which the AC current of the rectifier is estimated. Both the proposed controller and observer are assessed with simulation studies and the results show the acceptable performance of the observer and CCS-MPC as well as good disturbance rejection in load and network parameter variations.**

***Index Terms*—Continuous Control Set (CCS), Single-phase Rectifier, Model Predictive Control (MPC), Observer**

I. Introduction

Fundamentally, model predictive control solves an optimization problem by taking into account the future states and input in a moving horizon. In each sampling time, the next step is computed to drive the optimum operation of the system [1]- [2]. The predictive controller in power electronics used to be designed based on the switching nature of the plant [3]- [4]; indeed, the considered cost function is evaluated in all switching states, hence the switching state that minimizes the objective is selected in each sampling time for next action. This type of MPC is called finite control set (FCS) MPC; despite its simplicity, FCS-MPC suffers from variable switching frequency that does activate parasitic harmonics in waveforms [5]. However some papers reported how to mitigate the harmonic pollution, the filter design for this widespread harmonics would be an essential hindrance for FCS-MPC to be comprehensively used in practice [6]. Moreover, the computational load would be exponentially increasing for complicated converters with much more switching states [7]. The computational efficiency also would be extremely violated in a large prediction horizon. This paper introduces a continuous control set (CCS) MPC for for a single phase rectifier. CCS-MPC optimizes a cost function including predicted values of grid current and duty cycle variations [8]. The controller output is the optimum action that should be modulated with the PWM module. This type of MPC can manipulate a continuous duty cycle compared to FCS-MPC which has to work with limited switching states [9]- [10].

The DC bus voltage of the single-phase rectifier is measured and controlled with a PI controller in the outer loop, which is responsible for a sinusoidal grid current with an almost unity power factor. The grid current is not measured and is estimated by a full state observer and then controlled by the proposed CCS-MPC. The full state observer is designed to estimate both states of output voltage and grid current. There is a voltage sensor but the output voltage is estimated only for having a free noise voltage signal.

The rest of this paper is organized as follows. Section II presents the observer design. Section III explains the procedure for the proposed controller design. A PI controller is also designed for the voltage loop in this section. A comparison with FCS-MPC is performed in section IV, and finally, concluding remarks are provided in section V.

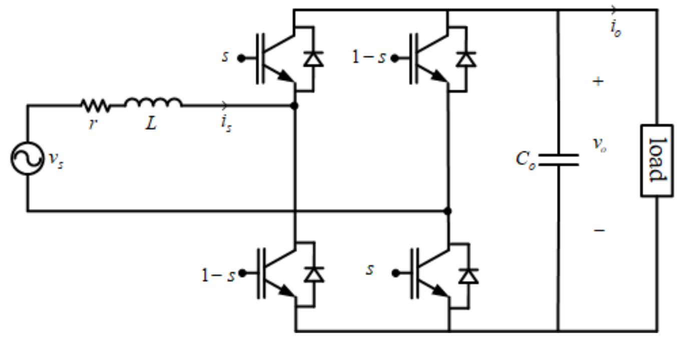

Fig. 1. Full bridge single-phase rectifier.

II. Observer Design

A single-phase full-bridge rectifier is shown in Fig. 1 where i_s and v_s are grid current and voltage, v_o is DC bus voltage and i_o is the load current. The equations below describe the rectifier switch model using a switching signal of s which can accept the integers 0 or 1.

$$\begin{cases} -v_s(t) + L\frac{di_s(t)}{dt} + ri_s(t) + (2s-1)v_o(t) = 0 \\ C_o\frac{dv_o(t)}{dt} - (2s(t)-1)i_s(t) + i_o(t) = 0 \end{cases} \quad (1)$$

The system of (1) can be arranged in a standard state-space form of:

$$\begin{cases} \dot{x}(t) = Ax(t) + Bv_s(t) + Ei_0(t)) \\ \\ y(t) = Cx(t) \end{cases} \tag{2}$$

where A, B, and C are state, input, and output matrices respectively. In addition, x is a two-dimensional vector including grid current and DC voltage. The selection of matrix C signifies that only the second state i.e. v_o is measured. The matrix E is the corresponding disturbance matrix due to load variations.

$$\begin{cases} A = \begin{bmatrix} \frac{-r}{L} & \frac{1-2s(t)}{C_0} \\ \\ \frac{2s(t)-1}{C_0} & 0 \end{bmatrix}, B = \begin{bmatrix} \frac{1}{L} \\ \\ 0 \end{bmatrix}, E = \begin{bmatrix} 0 \\ \\ \frac{-1}{C_0} \end{bmatrix}, \\ \\ C = [0 \quad 1] \end{cases} \tag{3}$$

As mentioned, in this work, the grid current is not measured. In general, for cascade control in power electronics, both states of voltage and current should be available for control purposes. However, measuring one state, the other state could be estimated; thus, for grid current estimation, an observer is designed based on the switch model of the rectifier. It increases the cost and space efficiency due to the lack of the need for current sensor.

$$\begin{cases} \dot{\hat{x}}(t) = A\hat{x}(t) + Bv_s(t) + Ei_0(t) + L_{ob}\left(y(t) - \hat{y}(t)\right) \\ \\ \hat{y}(t) = C\hat{x}(t) \end{cases} \tag{4}$$

The observer of (4) is running within the software in parallel with rectifier hardware. This is a full-state observer since the voltage of the DC bus is estimated too to eliminate the noise effect on the measurement side [11]. Since the rectifier state matrix of A has a compact bilinear form, first the observability of the plant should be verified in two switching states of 0 and 1.

$$ob = \begin{bmatrix} C \\ \\ CA \end{bmatrix} = \begin{bmatrix} 0 & 1 \\ \\ \frac{2s(t)-1}{C_0} & 0 \end{bmatrix} \tag{5}$$

$$\det(ob) = \begin{cases} \frac{1}{C_0} & s(t) = 0 \\ \\ \frac{-1}{C_0} & s(t) = 1 \end{cases} \tag{6}$$

The determinant value of the observability matrix is not zero for both switching states that denotes the matrix ob has full rank. Hence, by measuring output voltage, another state of the system can be theoretically estimated. The Ackermann formula is employed for obtaining observer gain as:

$$L_{ab} = [0 \quad 1][C^T \quad A^T C^T]^{-1}\alpha(A) \tag{7}$$

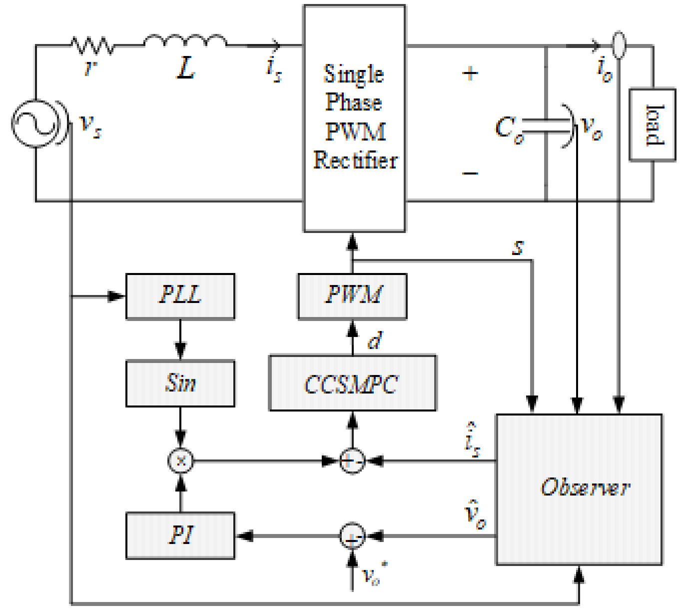

Fig. 2. Schematic of the proposed controller and observer.

where $\alpha(\lambda)$ is the desired dynamic of observer as bellow. The parameters λ_1 and λ_2 denote positions of observer eigenvalues for the characteristic equation of $\alpha(\lambda)$ in s-plane.

$$\alpha(\lambda) = (\lambda - \lambda_1)(\lambda - \lambda_2) \tag{8}$$

Using forward Euler, the discretized form of the observer is described in (9):

$$\begin{cases} \hat{x}(k+1) = T_s\left(A - L_{ob} + \frac{I_{2\times 2}}{T_s}\right)\hat{x}(k) + \\ \qquad T_s\left[Bv_s(k) + Ei_o(k) + L_{ob}y(k)\right] \\ \\ \hat{y}(k+1) = C\hat{x}(k) \end{cases} \tag{9}$$

III. Controller Design

The overall schematic of the controller is shown in Fig. 2. A PI controller is designed for the outer loop where the estimated voltage is compared with the required DC voltage in the output bus. For inner loop, a CCS-MPC is designed that the detailed steps are given as the following.

Supposing that the outer loop fixes the output voltage at a reference value of v_o^*, average model of the inner loop for the rectifier can be described as:

$$\frac{d\hat{i}_s(t)}{dt} = \frac{1}{L}\left(-r\hat{i}_s(t) - v_o^* d(t) + v_s(t)\right) \tag{10}$$

where d is the duty cycle and is defined as:

$$d(t) = 2s(t) - 1 \tag{11}$$

The small-signal model of the (12) is acquired using Taylor series expansion around the interest point of $v_o(t) = v_o^*$:

$$\frac{d\tilde{i}_s(t)}{dt} = \frac{1}{L}\left(-r\tilde{i}_s(t) - v_o^*\tilde{d}(t)\right) \quad (12)$$

The discretized small-signal model can be obtained as:

$$\tilde{i}_s(k+1) = \left(1 - \frac{T_s}{L}\right)\tilde{i}_s(k) - \frac{T_s}{L}v_o^*\tilde{d}(k) \quad (13)$$

The variation of the grid current is augmented to the state vector in (14) to benefit from integrator property in a steady-state.

$$\tilde{i}_s^a(k) = [\Delta\tilde{i}_s(k) \qquad \tilde{i}_s(k)]^T \quad (14)$$

where:

$$\Delta\tilde{i}_s(k) = \tilde{i}_s(k) - \tilde{i}_s(k-1) \quad (15)$$

Hence, the augmented state-space system can be described as:

$$\begin{cases} \tilde{i}_s^a(k+1) = A_a\tilde{i}_s^a(k) + B_a\Delta\tilde{d}(k) \\ \tilde{i}_s(k) = C_a\tilde{i}_s^a(k) \end{cases} \quad (16)$$

where:

$$\Delta\tilde{d}(k) = \tilde{d}(k) - \tilde{d}(k-1) \quad (17)$$

$$A_a = \begin{bmatrix} 1-\frac{T_s}{L} & 0 \\ 1-\frac{T_s}{L} & 1 \end{bmatrix}, B_a = -\frac{V_{dc}T_s}{L}\begin{bmatrix} 1 \\ 1 \end{bmatrix}, C_a = \begin{bmatrix} 0 & 1 \end{bmatrix} \quad (18)$$

Using (18), the predicted values of i_s^a can be computed as:

$$\begin{cases} \tilde{i}_s^a(k+2) = A_a^2\tilde{i}_s^a(k) + A_aB\Delta\tilde{d}(k) + B\Delta\tilde{d}(k+1) \\ \vdots \\ \tilde{i}_s^a(k+N_p) = A_a^{N_p}\tilde{i}_s^a(k) + \\ \qquad A_a^{N_p-1}B\Delta\tilde{d}(k) + A_a^{N_p-2}B\Delta\tilde{d}(k+1) \\ \qquad \cdots + A_a^{N_p-N_c}B\Delta\tilde{d}(k+N_c-1) \end{cases} \quad (19)$$

Hence,

$$\tilde{i}_s(k+N_p) = C_a\tilde{i}_s^a(k+N_p) \quad (20)$$

The parameters N_p and N_c are prediction and control horizons. By defining the vectors of (21) and (22), all the predicted states and output variables are described in a compact form of (23).

$$I_s = \left[\tilde{i}_s(k+1) \quad \tilde{i}_s(k+2) \quad \cdots \quad \tilde{i}_s(k+N_p)\right]^T \quad (21)$$

$$\Delta D = \left[\Delta\tilde{d}(k) \quad \Delta\tilde{d}(k+1) \quad \cdots \quad \Delta\tilde{d}(k+N_c-1)\right]^T \quad (22)$$

$$I_s = F\tilde{i}_s^a(k) + \Phi\Delta D \quad (23)$$

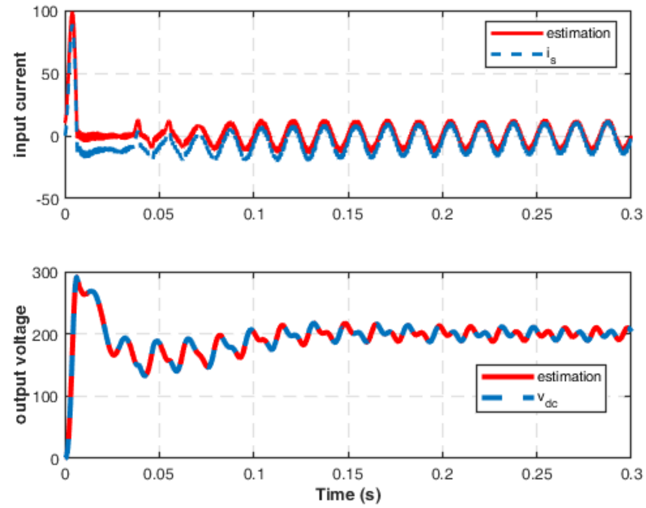

Fig. 3. Dynamic performance of the proposed observer.

where:

$$F = \left[C_aA_a \quad C_aA_a^2 \quad \cdots \quad C_aA_a^{N_p}\right]^T \quad (24)$$

$$\Phi = \begin{bmatrix} C_aB_a & 0 & \cdots & 0 \\ C_aA_aB_a & C_aB_a & \cdots & 0 \\ \vdots & \vdots & \cdots & 0 \\ C_aA_a^{N_p-1}B_a & C_aA_a^{N_p-2}B_a & \cdots & C_aA_a^{N_p-N_c}B_a \end{bmatrix} \quad (25)$$

The cost function of the MPC is described as (26). The minimization of this function will force the grid current to track the reference signal of the outer loop in the prediction horizon. In addition, the second term of the cost function includes the duty cycles variations to be minimized.

$$J = (I_s^* - I_s)^T(I_s^* - I_s) + \Delta D^T R_w \Delta D \quad (26)$$

where R_w is a weighting factor described by a diagonal matrix. Ultimately the optimum variation of the duty cycle yields:

$$\Delta D = \left(\Phi^T\Phi + R_w\right)^{-1}\Phi^T\left(I_s^* - F\tilde{i}_s^a(k)\right) \quad (27)$$

Afterward, the control sequence is computed within the control horizon where only the first action will be sent to manipulating variable [12].

IV. Simulation Results

In this section, the performance of the proposed controller and observer is examined with a simulation study. The observer gain is determined in such a way the observer performance should not have any frequency interference with the proposed controller. In Fig. 3, the systems states including input current and output voltages are depicted, which demonstrates suitable tracking of the measurements.

The controller is designed based on minimization of the cost function over $N_p = 1$. The other controller parameters are tuned based on try and errors to achieve the best output in steady state and parameters variations of the closed-loop system. In Fig. 4, the source voltage and current, and also output voltage are shown, which verify the adequacy of the proposed controller to regulate output voltage at $200\ V$. Since load variation is inevitable, hence the system performance is investigated during a disturbance in output load. However, the proposed control could preserve output voltage with an acceptable transient time. Furthermore, change in network parameters is also examined. In fact, during a variation in network inductor, the source voltage and current, and also output voltage are depicted in Fig. 5, which shows an acceptable performance to regulate output voltage. Line voltage and current are in phase with unity power factor.

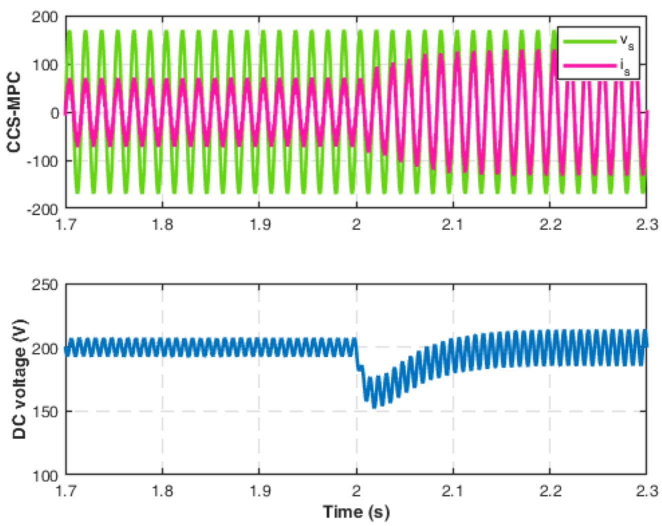

Fig. 4. System performance to the load disturbance

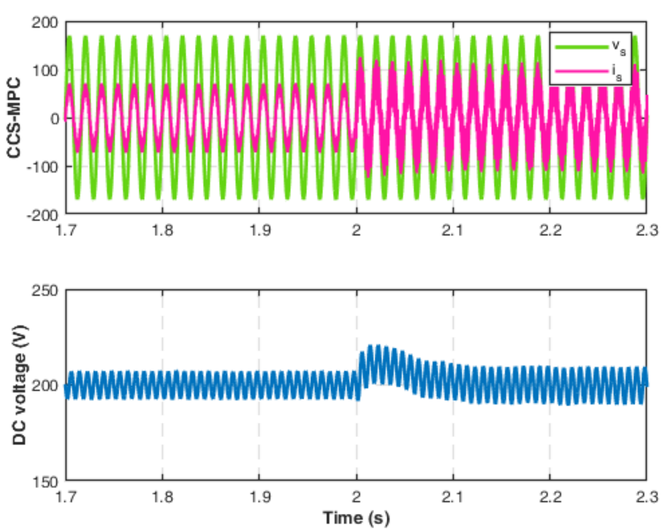

Fig. 5. System performance to the source disturbance

To prove the adequacy of our proposed controller, the proposed controller and observer should be compared with state of the art controllers in the literature. In our future work, a comparison study will be done to compare the performance of CCS-MPC and FCS-MPC to control a single phase rectifier.

V. Conclusion

The methodology of continuous control set MPC has been explained in detail for a single-phase rectifier. The proposed CCS-MPC works with a fixed switching frequency that simplifies the filter design for the measurement system. To help the system cost and space, a full-state observer is designed to omit a current sensor requirement for grid current measurement. The simulation results has demonstrated the CCS-MPC capability to provide unity power factor along with disturbance rejection in system parameters variations.

References

[1] L. Wang, *Model predictive control system design and implementation using MATLAB®*. Springer Science & Business Media, 2009.

[2] A. Kaymanesh, A. Chandra, and K. Al-Haddad, "Model predictive control of mpuc7-based statcom using autotuned weighting factors," *IEEE Transactions on Industrial Electronics*, vol. 69, no. 3, pp. 2447–2458, 2022.

[3] H. Kawai, Z. Zhang, R. Kennel, and S. Doki, "Direct speed control based on finite control set model predictive control with voltage smoother," *IEEE Transactions on Industrial Electronics*, vol. 70, no. 3, pp. 2363–2372, 2023.

[4] M. Babaie, M. Mehrasa, M. Sharifzadeh, and K. Al-Haddad, "Floating weighting factors ann-mpc based on lyapunov stability for seven-level modified puc active rectifier," *IEEE Transactions on Industrial Electronics*, vol. 69, no. 1, pp. 387–398, 2021.

[5] S. Vazquez, J. I. Leon, L. G. Franquelo, J. Rodriguez, H. A. Young, A. Marquez, and P. Zanchetta, "Model predictive control: A review of its applications in power electronics," *IEEE industrial electronics magazine*, vol. 8, no. 1, pp. 16–31, 2014.

[6] J. I. Leon, S. Kouro, L. G. Franquelo, J. Rodriguez, and B. Wu, "The essential role and the continuous evolution of modulation techniques for voltage-source inverters in the past, present, and future power electronics," *IEEE Transactions on Industrial Electronics*, vol. 63, no. 5, pp. 2688–2701, 2016.

[7] A. Sahli, F. Krim, A. Laib, and B. Talbi, "Model predictive control for single phase active power filter using modified packed u-cell (mpuc5) converter," *Electric Power Systems Research*, vol. 180, p. 106139, 2020.

[8] T. Brüdigam, D. Prader, D. Wollherr, and M. Leibold, "Model predictive control with models of different granularity and a non-uniformly spaced prediction horizon," in *2021 American Control Conference (ACC)*, 2021, pp. 3876–3881.

[9] A. Dehghanzadeh, G. Farahani, and M. Maboodi, "Maximum power point tracking of a photovoltaic system using modified incremental algorithm and model predictive control," *Journal of Control*, vol. 12, no. 2, 2018. [Online]. Available: http://joc.kntu.ac.ir/article-1-521-en.html

[10] F. Sebaaly, H. Y. Kanaan, J. Rodriguez, and K. Al-Haddad, "Direct predictive control for a nine-level packed e-cell (pec9) converter based shunt active power filter (sapf)," in *IECON 2021–47th Annual Conference of the IEEE Industrial Electronics Society*. IEEE, 2021, pp. 1–7.

[11] J. R. Rodriguez-Rodrıguez, E. L. Moreno-Goytia, V. Venegas-Rebollar, D. Campos-Gaona, R. A. Felix, and L. E. Ugalde-Caballero, "Current-sensorless control of an spwm h-bridge-based pfc rectifier designed considering voltage sag condition," *Electric Power Systems Research*, vol. 130, pp. 181–191, 2016.

[12] A. Dehghanzadeh, G. Farahani, H. Vahedi, and K. Al-Haddad, "Model predictive control design for dc-dc converters applied to a photovoltaic system," *International Journal of Electrical Power & Energy Systems*, vol. 103, pp. 537–544, 2018.